

# KINETIC ANALYSIS OF CHANNEL GATING

## Application to the Cholinergic Receptor Channel and the Chloride Channel from *Torpedo californica*

P. LABARCA,\* J. A. RICE,‡ D. R. FREDKIN,\* AND M. MONTAL\*§

Departments of \*Physics, ‡Mathematics, and §Biology, University of California, San Diego, La Jolla, California 92093

**ABSTRACT** Identification of the minimum number of ways in which open and closed states communicate is a crucial step in defining the gating kinetics of multistate channels. We used certain correlation functions to extract information about the pathways connecting the open and closed states of the cation channel of the purified nicotinic acetylcholine receptor and of the chloride channel of *Torpedo californica* electroplax membranes. Single channel currents were recorded from planar lipid bilayers containing the membrane channel proteins under investigation. The correlation functions are conveniently computed from single channel current records and yield information on  $E$ , the minimum number of entry/exit states into the open or closed aggregates.  $E$  gives a lower limit on the numbers of transition pathways between open and closed states. For the acetylcholine receptor, the autocorrelation analysis shows that there are at least two entry/exit states through which the open and closed aggregates communicate. The chloride channel fluctuates between three conductance substates, here identified as C, M, and H for closed, intermediate, and high conductance, respectively. Correlation analysis shows that  $E$  is  $\geq 2$  for the M aggregate, indicating that there are at least two distinct entry/exit states in the M aggregate. In contrast, there is no evidence for the existence of more than one entry/exit state in the C or H aggregates. Thus, these correlation functions provide a simple and general strategy to extract information on channel gating kinetics.

### INTRODUCTION

A new approach for the kinetic analysis of channel gating is presented. Whereas the, by now, traditional method of analysis focuses on the forms of the distribution of open and closed dwell times, we have attempted to extract additional information about the structure of the kinetic system by considering certain aspects of the time history of the experimental records, in particular, dependencies between successive events. This approach, applied to the acetylcholine receptor channel (AChR) and the  $\text{Cl}^-$  channel of *Torpedo californica* electroplax, provides new information concerning the identification of states and about the pathways connecting the different states, thereby establishing a firmer basis for the proposal of specific mechanistic schemes.

In recent years, the technology has been developed to incorporate and reconstitute membrane channel proteins into planar lipid bilayers. These systems are ideally suited to perform electrical measurements with the sensitivity and time resolution necessary to record the opening and closing

of individual channels (Montal et al., 1981). The advent of the patch-clamp recording technique (Hamill et al., 1981) and its explosive application in electrophysiology is leading to the identification and characterization of a large number of ion channels. The combination of these two endeavors is generating a wealth of phenomenological information on the activity of channel proteins at the level of single molecular events.

Single channel recordings are especially amenable for detailed statistical analysis. Thus far the major analytical tool has been the computation of distributions, namely, the dwell times (lifetimes) in the open state and in the closed state of the channel. This analysis provides information about the number of open or closed states but gives no clue about the pathways to enter or exit from such states. We have developed an approach to the analysis of single channels that, in addition to one-dimensional distributions, takes advantage of autocorrelation and autocovariance functions in order to extract information about the pathways connecting the open and closed states (Fredkin et al., 1985). This approach is only appropriate for the analysis of stationary processes in membranes containing a single channel.

Here we apply this approach to two well-characterized membrane channel proteins from the electric organ of

---

Address all correspondence to Dr. M. Montal.

Dr. P. Labarca's present address is Laboratorio de Neurofisiologia, Universidad Catolica de Chile, Casilla 114-D, Santiago, Chile.

*Torpedo californica*. (a) The nicotinic cholinergic receptor channel (AChR): It is the most extensively characterized membrane channel protein from nervous systems. The AChR was purified from electroplax membrane vesicles and shown to be composed of five polypeptide components ( $\alpha_2\beta\gamma\delta$ , protein mol wt ~270,000) (for reviews see Changeux, 1981; Conti-Tronconi and Raftery, 1982; Karlin, 1983; Anholt et al., 1984). The purified AChR was reconstituted in planar lipid bilayers and shown to exhibit the characteristic properties of the postsynaptic receptor (Nelson et al., 1980; Boheim et al., 1981; Labarca, 1984a, b). The AChR channel undergoes rapid transitions between two well-defined conductance states, open and closed (but see Hamill and Sakmann, 1981; and Auerbach and Sachs, 1984).

(b) The chloride channel ( $\text{Cl}^-$  channel): This channel appears to be derived from the noninnervated face of the electroplax cell membrane and is highly selective for  $\text{Cl}^-$  ions (White and Miller, 1979, 1981; Miller and White, 1980; Miller, 1982; Hanke and Miller, 1983; Tank et al., 1982). The  $\text{Cl}^-$  channel is assayed by the incorporation of electroplax membrane vesicles into planar lipid bilayers (Miller, 1982). The  $\text{Cl}^-$  channel undergoes rapid transitions between three well-defined conductance states and, therefore, offers a system to apply our analysis to a channel that exhibits more than two states.

An extended account of the theoretical formalism discussed in this work (Fredkin et al., 1985) and a preliminary report of the experimental results (Labarca et al., 1984c) were presented elsewhere.

## MATERIALS AND METHODS

### AChR Preparation

Receptor from the electric organ of *Torpedo californica* (Pacific Bio-Marine Laboratories, Inc., Venice, CA) was solubilized, purified, and reconstituted in lipid vesicles as described in detail elsewhere (Nelson et al., 1980; Anholt et al., 1981, 1982). Analysis on sodium-dodecyl sulfate polyacrylamide gel electrophoresis shows that this preparation is composed of the four polypeptide subunits characteristic of the AChR ( $\alpha_2\beta\gamma\delta$ ). The functional integrity of the AChR in the reconstituted vesicles was assayed by the carbamylcholine-induced  $^{22}\text{Na}^+$ -uptake (Huganir et al., 1979; Anholt et al., 1981, 1982) before the electrical measurements.

### Planar Lipid Bilayers

Monolayers were derived from the reconstituted vesicles (Schindler and Quast, 1980) as described by Nelson et al. (1980) and Labarca et al. (1984a, b). Planar bilayers were assembled from two monolayers across a 200  $\mu\text{m}$  diameter hole pierced through a 12  $\mu\text{m}$  thick Teflon partition separating two 1-ml capacity Teflon chambers (Montal, 1974; Labarca et al., 1984a, b) or at the tip of a patch pipette, as described in detail elsewhere (Suarez-Isla et al., 1983). For the studies of the AChR channel, the aqueous medium was 0.5 M NaCl, 5 mM  $\text{CaCl}_2$ , 2.5 mM HEPES, pH 7.4, and 20 mM KSCN. At this  $\text{SCN}^-$  concentration, the  $\text{Cl}^-$  channel is blocked (White and Miller, 1981). The AChR channel was activated with ACh at the indicated concentration. The recordings of the  $\text{Cl}^-$  channel were obtained under the same conditions but KSCN and cholinergic agonists were omitted. The recordings of the AChR channels

were obtained at 100 mV. At this voltage the frequency of transitions between conductive states of the  $\text{Cl}^-$  channel is minimized since its probability of being open is virtually 1.0. Likewise, the records of  $\text{Cl}^-$  channels were performed at negative voltage to maximize the frequency of transitions between states (Miller, 1982). The  $\text{Cl}^-$  channel protein appears to copurify with the AChR protein as a minor constituent of the preparation ( $\leq 1\%$  detection level of contaminants with silver stain gels; Merrill et al., 1981). All experiments were performed at room temperature.

## Electrical Recordings

Single channel current recordings were obtained using techniques described in detail elsewhere (Labarca et al., 1984a, b; Suarez-Isla et al., 1983). Constant voltage was supplied by a variable direct current (DC) source, and the *trans* side of the membrane (opposite to that where agonist was added) was defined as zero voltage. Thus, a negative applied voltage corresponds to a depolarization in the electrophysiological convention. The output of the current to voltage converter was recorded on FM tape (RACAL 4DS, bandwidth DC to 5 kHz; Racal Recorders Ltd., Hythe, Southampton, England).

## Data Processing

After filtering at 2 kHz, the data were digitized at a sampling interval of 100  $\mu\text{s}$  for AChR data and 50  $\mu\text{s}$  for  $\text{Cl}^-$  channel data. Conductance levels were discriminated using a PDP 11/34A computer (Digital Equipment Corp., Marlboro, MA), as described in detail elsewhere (Labarca et al., 1984a). A VAX 11/750 computer (Digital Equipment Corp.) was used for statistical analysis of the data. Interactive data analysis used S, a computer package for data analysis, statistics, and graphics (Becker and Chambers, 1984), and curve fitting used MINPACK routines from SLATEC (National Energy Software Center, Argonne, IL)<sup>1</sup> to minimize the modified  $\chi^2$  statistic

$$\sum \frac{[N_{\text{obs}} - N(\mathbf{v})]^2}{N_{\text{obs}}}, \quad (1)$$

where  $N_{\text{obs}}$  is observed and  $N(\mathbf{v})$  is expected for the parameter vector  $\mathbf{v}$ . There was evidence for distortion of the distribution of dwell times at short times owing to the finite bandwidth of the electronics and the finite sampling rate in the analog-to-digital (A/D) conversion. Therefore, only dwell times that were 10 or more sampling intervals long were used to fit the one-dimensional distributions.

## THEORETICAL CONSIDERATIONS

In this section we briefly review some of the results of Fredkin et al. (1985). Further results and derivations are contained in that paper. Channel gating kinetics are modeled as stationary Markov process in continuous time with a finite state space. The states are classified into observable aggregates: for the AChR, there are two aggregates, open and closed, and for the  $\text{Cl}^-$  channel there are three aggregates, one closed and two open. Each of the aggregates may contain one or more states, and the inferential problem is to deduce from observation of the aggregated process the structure and perhaps transition rates of the underlying Markov process. In general, it may not be possible to do this in full, although some aspects of the structure may be deducible.

## One-dimensional Distributions

The observational data consists of a sequence of dwell times in the different aggregates, and all the information about the underlying process

<sup>1</sup>We used a locally modified (by D. R. Fredkin) version of SLATEC suitable for use under the UNIX operating system. UNIX is a trademark of Bell Laboratories.

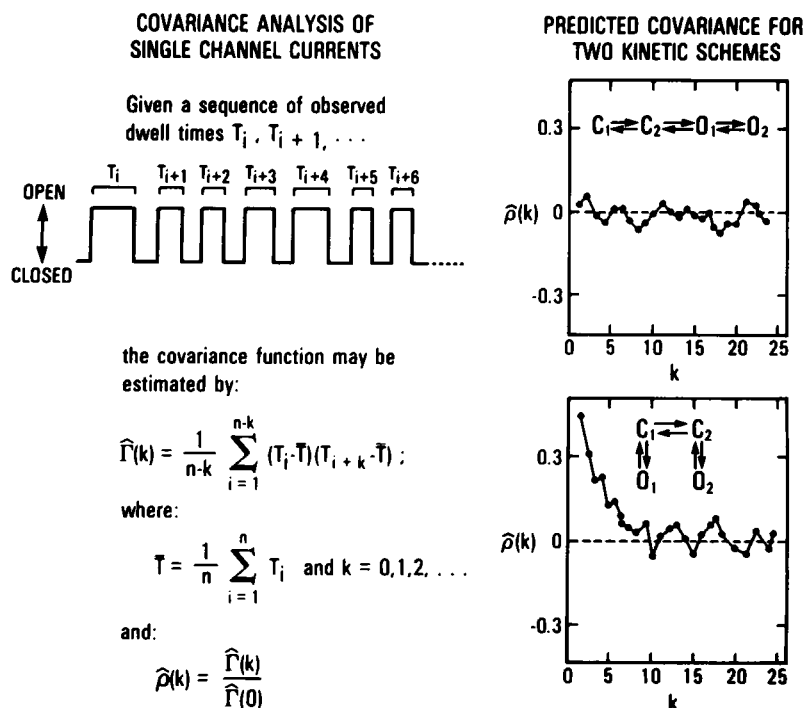


FIGURE 1 Schematic (idealized) representation of covariance analysis of single channel currents and the predicted covariance of the open state for two kinetic schemes. Notice that both schemes will give two open states in a one-dimensional (lifetime) distribution analysis but not in a covariance analysis. The roughness of the functions intends to convey the fluctuations due to sampling error that arise from using a finite amount of experimental data. The theoretical covariance functions are smooth.

is contained in the joint probability law of such sequences. The joint probability law was shown to be completely determined by the probability law of successive pairs of dwell times (actually, only the case of two aggregates is treated therein, but it can be shown that the same phenomena occur in general; Fredkin et al., 1985). Therefore, analysis of the joint distribution of successive pairs of dwell times can, in principle, extract all the obtainable information about the transition rates of the underlying process.

Important, but limited, information is traditionally extracted from experimental data from an analysis of one-dimensional distributions, for example, the probability distribution of the open dwell times. It is shown in Colquhoun and Hawkes (1981) that a one-dimensional distribution of dwell times has the form of a sum of exponentials and that the number of summands gives a lower bound on the number of states in the corresponding aggregate. This information, although extremely useful, gives no clues as to how these states are connected together or as to how they are connected to states in other aggregates.

As mentioned, dwell times of duration  $< 10$  sampling intervals were not used in fitting one-dimensional distributions. If there were relatively fast time constants, they would have been missed in the analysis and their presence would have biased the fitted values of slower time constants. It is quite possible that short open times were missed since the data are noisy and discretely sampled. Missing a short open time, for example, could result in a long apparent closed time and vice versa. The net effect on the analysis is not completely clear to us. This problem, which pervades all studies of this type, has not been extensively addressed in the literature.

### Autocorrelation Analysis

Information about the connectivity of the aggregates is contained in autocovariance or autocorrelation functions, which we will now describe. We assume that the process is stationary in time. For a particular aggregate, denote the sequence of successive dwell times in that aggregate

by  $T_1, T_2, T_3, \dots$  (Fig. 1). This is a stationary sequence, and has a covariance function

$$\Gamma(k) = \text{Cov}(T_i, T_{i+k}). \quad (2)$$

Note that this is a covariance of successive dwell times (not successive current samples). We also work with the correlation function

$$\rho(k) = \frac{\Gamma(k)}{\Gamma(0)}. \quad (3)$$

In the aggregate there are certain states, which we call entry/exit states, through which the aggregate communicates with the other aggregates. Denote the number of such states by  $E_1$ . Similarly, in the other aggregates there are entry/exit states through which they communicate with the aggregate of interest. Denote the number of these by  $E_2$ . Let  $E$  be the smaller of  $E_1$  and  $E_2$ . Theorem 5.1<sup>2</sup> of Fredkin et al. (1985) states that there exist  $u_i$  and  $\kappa_i$ ,  $0 \leq \kappa_i < 1$ , such that

$$\Gamma(k) = \sum_{i=1}^{E-1} u_i \kappa_i^{|k|}, \quad (4)$$

for  $k \neq 0$ .  $\Gamma$  is thus a sum of geometrically decaying components.

The practical importance of this result is that a lower bound for  $E$  is, in principle, obtainable from the covariance or correlation function, and provides information about the complexity of the intercommunication between different aggregates. At the simplest level, if  $E = 1$ , no

<sup>2</sup>There the quantities  $E_1$ ,  $E_2$ , and  $E$  were called  $M_1$ ,  $M_2$ , and  $M$ , respectively. We have changed notation to avoid conflict with the designation  $M$  for the intermediate conductance aggregate of the chloride channel.

correlation will be present. This may occur because there is only one entry/exit state in the aggregate or because there is only one entry/exit state in the other aggregates. However, note that if  $u_i$  or  $\kappa_i$  are 0, no correlation will be present (see Fig. 1).

It is easy to estimate a correlation function from data. If the sequence of observed dwell times is  $T_1, T_2, \dots, T_n$ , the covariance function may be estimated by

$$\hat{\Gamma}(k) = \frac{1}{n-k} \sum_{i=1}^{n-k} (T_i - \bar{T})(T_{i+k} - \bar{T}), \quad (5)$$

where

$$\bar{T} = \frac{1}{n} \sum_{i=1}^n T_i. \quad (6)$$

The correlation function  $\rho(k)$  is estimated by  $\hat{\rho}(k) = \hat{\Gamma}(k)/\hat{\Gamma}(0)$ .

Experimental records do not contain perfect measurements of the succession of dwell times,  $T_i$ . The data are noisy and discretely sampled and there is always the possibility that more than one channel is present. Some of the effects on the measured correlation structure can be analyzed. They certainly do not produce a non-null correlation structure. Here we take the conservative approach of drawing inferences only from indications of non-null correlation structure. Where nontrivial correlation was found, we did not attempt to fit Eq. 4 to it; only the existence of correlation was used.

## RESULTS

### AChR Channel

Fig. 2 shows single channel currents recorded from a planar lipid bilayer containing purified AChR activated by ACh at the concentration of 50  $\mu$ M. As indicated in the figure, the currents flowing through the individual channels appear at discrete transient steps that fluctuate between two identifiable levels: the closed and open states of the channel. A conductance histogram computed from such a record displays two distinct Gaussian distributions, corresponding to the current levels of the closed and open states. The single channel conductance estimated from the conductance histograms was 45 pS at 0.5 M NaCl. Single channel current records where only one channel was open at any given time were analyzed.

### One-dimensional Distribution

Tables I and II present the result of conventional analysis of the one-dimensional probability densities of dwell times

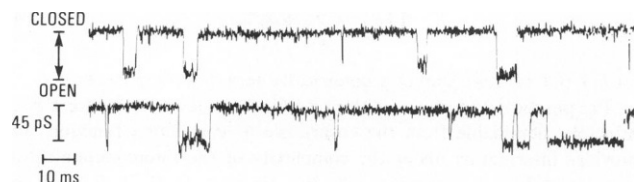


FIGURE 2 Single AChR channel currents activated by acetylcholine (50  $\mu$ M) at an applied voltage of -100 mV. The recordings were obtained from a bilayer formed at the tip of a patch pipette. The seal resistance was 5 G $\Omega$ . The record was low-pass filtered at 2 kHz. As indicated, a downward deflection corresponds to a channel opening event. The single channel conductance was in this particular record 50  $\pm$  5 pS.

TABLE I  
ONE-DIMENSIONAL PROBABILITY DENSITIES OF  
DWELL TIMES IN THE OPEN STATE OF THE AChR;  
NUMBER OF EXPONENTIAL COMPONENTS

Number of exponentials	Degrees of freedom	$\chi^2$	$p^*$
1	161	393.8	0.0000
2	159	201.9	0.0121
3	157	138.8	0.8882

Acetylcholine concentration was 50  $\mu$ M and the applied voltage was +100 mV. All dwell times <10 sampling intervals were discarded. The number of sampling intervals is equal to the number of degrees of freedom plus twice the number of exponentials.

\*If the number of exponentials is correct, the probability that  $\chi^2$  would be larger than the observed value is  $p$  (from the  $\chi^2$  distribution with the indicated number of degrees of freedom). A model would be statistically rejected at level  $\alpha$  (e.g.,  $\alpha = 0.05$ ) if  $\alpha > p$ .

in the open state of the AChR. Table I shows the quality of fit possible with sums of various numbers of exponentials, measured by the value of  $\chi^2$ . Specifically, a histogram of dwell times, normalized to have total area equal to one, is fitted as described under Methods, by a probability density of the form

$$f(t) = \sum_{i=1}^N A_i e^{-t/\tau_i}. \quad (7)$$

If we adopt a 5% significance level ( $p \leq 0.05$ ), we see that the open aggregate consists of at least three states. Table II gives the actual values of the time constants and prefactors for the acceptable fit with a sum of three exponentials. This new information was derived from the expansion of the one-dimensional probability density analysis to longer dwell times than we had previously attained (see Labarca et al., 1984a).

### Autocorrelation Analysis

Fig. 3 shows the correlation function for the open aggregate of the AChR channel. Since the estimates are computed from finite stretches of data, they are subject to random variability, and must be interpreted with this in mind. In the case of white noise (a time series of independent and identically distributed observations, and thus with

TABLE II  
ONE-DIMENSIONAL PROBABILITY DENSITIES OF  
DWELL TIMES IN THE OPEN STATE OF THE AChR;  
PARAMETERS OF EXPONENTIAL COMPONENTS

Time constant	Prefactor
ms	ms <sup>-1</sup>
48.73	0.003028
5.828	0.09768
0.6496	0.8408

Acetylcholine concentration was 50  $\mu$ M and the applied voltage was +100 mV.

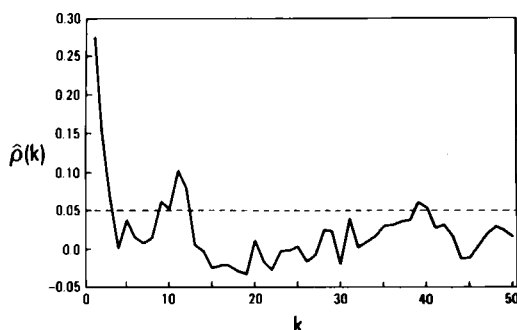


FIGURE 3 Autocorrelation function for the open aggregate of the AChR channel. The dashed horizontal lines are at  $\pm 2\sqrt{n}$ , i.e., plus and minus twice the approximate standard error of the estimate in the case of white noise. Acetylcholine concentration was  $50 \mu\text{M}$  and the applied voltage was  $100 \text{ mV}$ . The total number of openings in this analysis was 1,600. The origin of the bump near  $k = 12$  is not entirely clear. It appears to be caused by two very long openings separated by 11 shorter ones. Note that the estimates of  $\hat{\rho}(k)$  for different  $k$  are correlated, so the anomaly has an extended width.

$\rho(k)=0$  for  $k \neq 0$ ) the correlation function estimates are approximately normally distributed with mean zero and variance  $1/n$ , where the observed series is of length  $n$  (Cox and Lewis, 1966). Since the theory described above states that the correlation function decays geometrically, we focus attention on the correlation function near zero and only consider a correlation significant if it is larger in absolute value than  $2/\sqrt{n}$ .

As seen in Fig. 3, substantial correlation is present, and the correlation at small lags is stronger than that observed in the  $\text{Cl}^-$  channel (see Fig. 6). We have not attempted to fit the correlation function with geometrically decaying components; it is not clear whether there is sufficient resolution to allow discrimination between one and two components, and the appropriate statistical tests are more complicated than the chi square tests used to determine the number of components in the one-dimensional distribu-

tions. Thus, it is clear that there are at least two entry/exit states through which the open and closed aggregates communicate.

### Chloride Channel

Fig. 4 illustrates single channel records of the  $\text{Cl}^-$  channel obtained at three different applied voltages:  $-80$ ,  $-120$ , and  $-180 \text{ mV}$ . As originally reported by White and Miller (1979) and Miller (1982) the  $\text{Cl}^-$  channel is voltage dependent. At  $-80 \text{ mV}$ , three distinct conductance levels are distinguishable: a low conductance level, here denoted as C, an intermediate conductance level, identified as M, and a high conductance level, defined as H. The channel fluctuates between the three substates with apparent conductances of 0, 16, and  $32 \text{ pS}$  in  $0.5 \text{ M Cl}^-$ . Transitions between the three states are observed at  $-120$  and  $-180 \text{ mV}$ . Notice, however, that the probability of occurrence of the different states varies with the applied voltage. At  $-80 \text{ mV}$  the most populated state is H, while the frequency of occurrence of the C state is very low. As the voltage is made more negative, the probabilities of occurrence of the M and C states increased progressively, at the expense of the H-state probability. This is clearly illustrated in Fig. 5, where a conductance histogram is shown: Three distinct Gaussian distributions are evident corresponding to the current levels of the C, M, and H states. The single channel conductances are readily estimated from the difference of the current at the peaks of the distributions divided by the applied voltage. The left-hand panel is the conductance histogram for the recording obtained at  $-80 \text{ mV}$ . Two distinct peaks corresponding to the H and M states are identified, whereas that corresponding to the C state is not discernable. In contrast, at  $-180 \text{ mV}$  three distinct peaks are observed where the probability of occurrence of the C state increases at the expense of the H state. An intermediate situation is presented at  $-120 \text{ mV}$ , where the C state

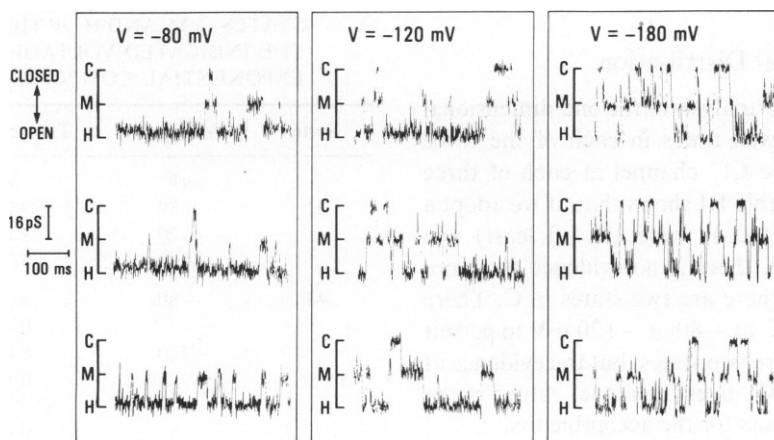


FIGURE 4 Single  $\text{Cl}^-$  channel records obtained at  $-80$ ,  $-120$ , and  $-180 \text{ mV}$ , respectively. The bilayers were formed across an aperture in a Teflon partition separating two aqueous chambers. Three contiguous sections of the records at each voltage are illustrated. The three conductance states C, M, and H are indicated with the corresponding conductances of 0, 16, and  $32 \text{ pS}$ . A downward deflection corresponds to and increase in membrane conductance. All the records were low-pass filtered at  $2 \text{ kHz}$ .

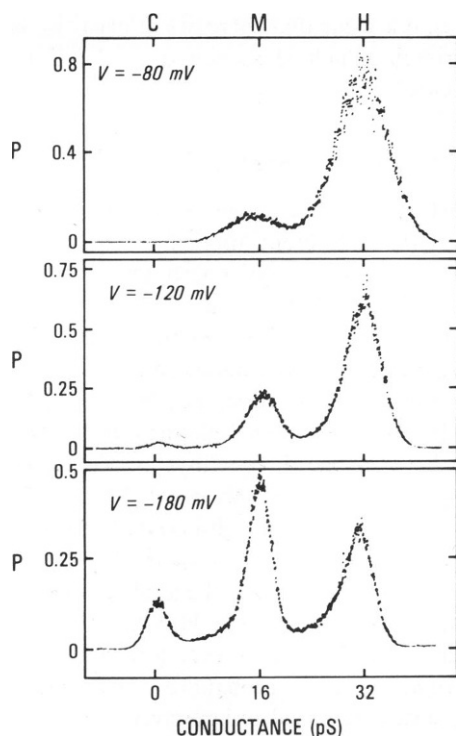


FIGURE 5 Single  $\text{Cl}^-$  channel conductance histograms. The histograms are plots of the frequency of occurrence of a given current level. The upper panel is the conductance histogram obtained at  $-80$  mV, the middle panel is that for the recording obtained at  $-120$  mV, and the lower panel corresponds to the  $-180$ -mV record. Three Gaussian distributions are clearly discerned in the latter record; the first one with a mean value  $\sim 0$  current, the second with a peak  $\sim 16$  pS, and the third peak  $\sim 32$  pS. The three peaks correspond to the conductance associated with the C, M, and H states, respectively. The relative areas under the curves are proportional to the probability of occurrence of each state at the indicated voltage.

is populated at the expense of the H state. These observations agree well with those previously reported by Miller and collaborators (White and Miller, 1981; Miller, 1982; Hanke and Miller, 1983).

### One-dimensional Distribution

Tables III and IV show the analysis of the one-dimensional probability densities of dwell times in each of the three states C, M, and H of the  $\text{Cl}^-$  channel at each of three representative voltages. Table III shows that, if we adopt a 5% significance level ( $p \leq 0.05$ ), there are (at least) two states in the aggregate M, there is no evidence for more than one state in H, and there are two states in C. There are two few transitions to C at  $-80$  or  $-120$  mV to permit the conclusion that there are two states, but the evidence at  $-180$  mV is clear. Table IV gives the actual values of the time constants and prefactors for the acceptable fits.

### Autocorrelation Analysis

Fig. 6 shows the estimated correlation functions for the aggregates C, M, and H for each of the three voltages. The

TABLE III  
ONE-DIMENSIONAL PROBABILITY DENSITIES OF DWELL TIMES IN EACH OF THE THREE STATES C, M, AND H OF THE  $\text{Cl}^-$  CHANNEL AT THE INDICATED VOLTAGE; NUMBER OF EXPONENTIAL COMPONENTS

State	Voltage	Number of exponentials	Degrees of freedom	$\chi^2$	$p^*$
	mV				
H	-80	1	332	243.2	0.9999
	-120	1	323	284.1	0.9418
	-180	1	227	200.6	0.8960
M	-80	1	181	253.3	0.0003
		2	179	187.2	0.3220
	-120	1	210	384.0	0.0000
		2	208	189.0	0.8234
	-180	1	225	690.4	0.0000
		2	223	166.4	0.9982
C	-80	1	18	10.71	0.9063
	-120	1	36	40.47	0.2795
	-180	1	73	447.0	0.0000
		2	71	43.90	0.9953

All dwell times  $< 10$  sampling intervals were discarded.

\*If the number of exponentials is correct, the probability that  $\chi^2$  would be larger than the observed value is  $p$  (from the  $\chi^2$  distribution with the indicated number of degrees of freedom).

only significant correlation function in the figure is for aggregate M at  $-180$  mV. The correlation functions for aggregate M at  $-80$  and  $-120$  mV are not significantly different from 0. This does not mean that they are, in fact, 0 but only that they appear to be small enough to be indistinguishable from the noise level. Fig. 5 indicates one reason for the lack of observed correlation at these two voltages: there are relatively few transitions from aggregate

TABLE IV  
ONE-DIMENSIONAL PROBABILITY DENSITIES OF DWELL TIMES IN EACH OF THE THREE STATES C, M, AND H OF THE  $\text{Cl}^-$  CHANNEL AT THE INDICATED VOLTAGE; PARAMETERS OF EXPONENTIAL COMPONENTS

State	Voltage	Time constant	Prefactor
	mV	ms	$\text{ms}^{-1}$
H	-80	29.02	0.03334
	-120	14.22	0.06624
	-180	5.730	0.1714
M	-80	4.762	0.1820
		0.4533	0.7328
	-120	6.428	0.1272
		0.1967	7.730
	-180	6.750	0.09984
		0.4292	2.156
C	-80	2.351	0.4864
	-120	3.782	0.2712
	-180	7.711	0.1820
		0.3245	7.202

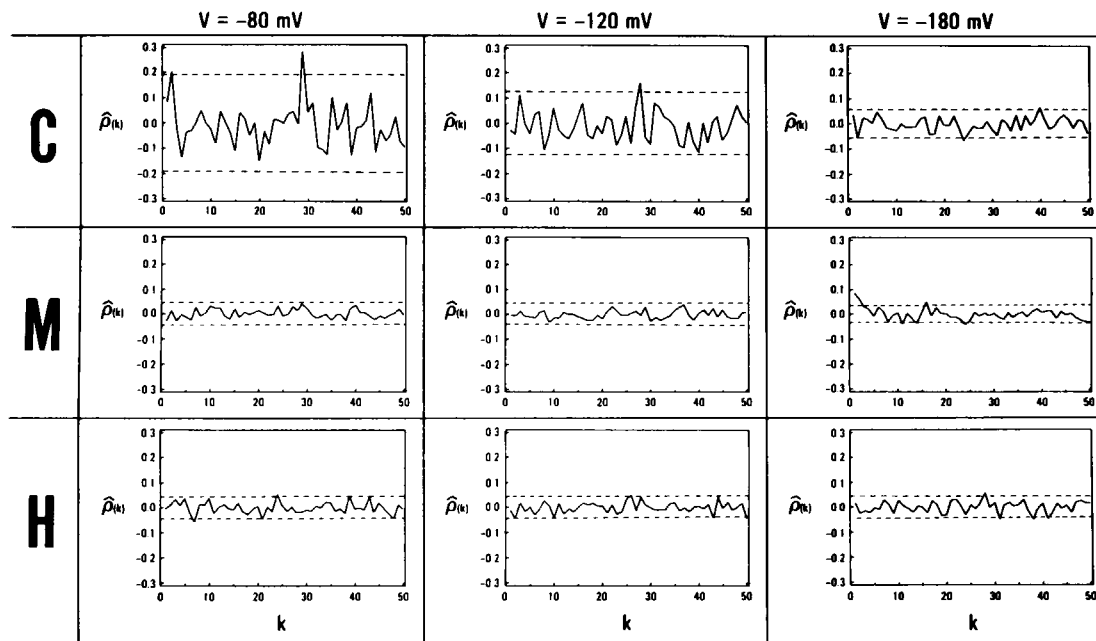


FIGURE 6 Autocorrelation functions for the C, M, and H aggregates (rows) at  $-80$ ,  $-120$ , and  $-180$  mV (columns). The dashed horizontal lines are at plus and minus twice the approximate standard errors of the estimates in the case of white noise. The number of openings corresponding to each plot are given as follows: for state C at  $V = -80$ ,  $-120$ , and  $-180$  mV the corresponding openings are 116, 260, and 1,189, respectively; in states M and H at the same  $V$  values the corresponding openings are 2,066, 2,500, and 3,086, respectively, in state M and 2,066, 2,268, and 2,066 in state H.

gate C to aggregate M. At  $-180$  mV, there are enough transitions into/from M from/into both C and H to show that there are at least two distinct entry/exit states in the M aggregate. Data obtained at  $-160$  mV, not reported for considerations of space, all show correlation. The correlation functions for aggregates C and H are indistinguishable from 0 at all voltages. This is consistent with a model in which there is only one entry/exit state in each of these aggregates.

### Further Analysis of Transition Histories

The dwell times in M can be classified into four types, depending on whether they were preceded or followed by sojourns in C or H. To gain some qualitative insight into the nature of the transition mechanisms, these four sets of dwell times are compared in Fig. 7 at each of the three voltages by means of box plots. A box plot of a batch of numbers is constructed in the following way: A box is

drawn that contains the central 75% of the data, and a line at the median is drawn in the box. "Whiskers" are drawn from the edges of the box out to the nearest data points within a distance of 1.5 times the interquartile range. Points beyond the whiskers are indicated by asterisks. Finally, the width of the box is proportional to the square root of the number of observations. Thus, a box plot constructed from the log dwell times is a convenient summary of the center, spread, and asymmetry of the distribution of the data values, and of the presence of extreme observations.

Fig. 7 illustrates that, at the less negative voltages, most of the sojourns in M are preceded and followed by sojourns in H. Further, as the voltage becomes more negative, most of the sojourns in M that are preceded and followed by sojourns in H become shorter in duration than the other sojourns; note, however, that there are a relatively large number of such dwell times at  $-180$  mV that are separated from the body of the other dwell times, as indicated

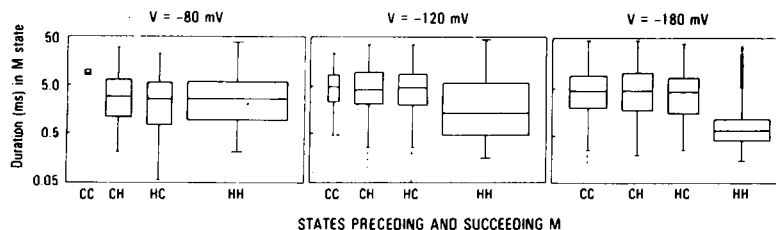


FIGURE 7 Box plots of dwell times in M classified into four types, depending on whether they were preceded or followed by sojourns in C or H, at  $-80$ ,  $-120$ , and  $-180$  mV. The construction of the box plots is discussed in the text.

by the blur of asterisks. The following is a possible explanation. Suppose that there is a state in M through which transitions to and from H occur and that the transition rate to H from this state is especially voltage sensitive. Then, at large negative voltages when the process exits from H and enters this state it is likely to return to H very quickly without visiting any other states in M; the body of the data consist of dwell times of this type. Some small fraction of the time, however, upon leaving it, the process either exits to a different M state, or exits to the voltage-sensitive M state and then leaves this state for other M states to finally return to H. These dwell times are typically much longer and correspond to the blur of asterisks.

The box plots also reinforce a conclusion reached from examination of the correlation functions: if there were only one entry/exit state in M, the box plots would look identical (apart from sampling error), and instead we see a clear indication of more complexity in the interaggregate structure.

The general analysis in Fredkin et al. (1985) indicates that information about an aggregated system may be contained in two-dimensional distributions, for example, the joint distribution of dwell times in M and succeeding dwell times in H. Fig. 8 is a scatterplot of such pairs of dwell times at  $-180$  mV, in which there is no apparent dependency; this is to be expected if H and M are linked by a single state since, in that case, the dwell time in M is independent of the succeeding dwell time in H. This result (and others not presented for considerations of space) supports the conclusion based on the correlation functions that there is no evidence for the existence of more than one entry/exit state in C or in H. This is consistent with the one-dimensional distribution of dwell times in H, which were shown above to be well fitted by a single exponential. The one-dimensional analysis of C required fitting two exponentials giving information about the complexity of C, but could not yield information about the complexity of intercommunication between C and M.

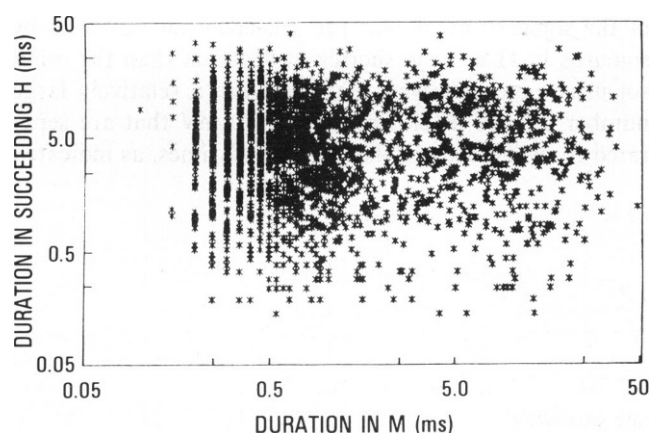


FIGURE 8 Scatter plot of the dwell times in H vs. the preceding dwell times in M at  $-180$  mV.

We note that the correlation analysis and transition history analysis shown in Figs. 6 and 7 are inconsistent with the model proposed by Miller (1982) in which the channel consists of two simple identical pathways in parallel, each consisting of an open and closed state, since for this model the correlation functions should all be null. A detailed analysis of this model is provided in the Appendix.

## DISCUSSION AND CONCLUSIONS

The analysis of single channel currents of the purified AChR performed by Labarca et al. (1984a) provided evidence for the existence of two open states. The analysis applied here further supports that notion and, in addition, indicates that these two open states can be entered or exited via at least two pathways. This new information was extracted from the autocovariance analysis and it is an independent demonstration for the existence of, at least, two open states. Jackson et al. (1983), studying the AChR channel in cultured cells, applied a different correlation test based on the analysis of pairs of openings and reached a similar conclusion. The evidence provided here obtained from autocovariance functions is of a more general nature: it provides evidence for the existence of at least two open states and it also indicates that the two open states can be reached from at least two closed states.

In addition, the extension of the one-dimensional analysis to longer dwell times than previously available revealed the existence of yet another component of the distribution of open time durations. This result may have significant implications in the evaluation of current models of the AChR channel operation. The analysis described here extended to a wide range of agonist concentrations may provide some insights into the correlation between agonist binding and channel opening (Labarca, P., and M. Montal, unpublished work).

Studies on the kinetics of gating of the  $\text{Cl}^-$  channel led Miller and collaborators (Miller, 1982; Miller and White, 1984) to suggest that the channel consists of two subunits, with identical conductance and kinetics, that open independently of each other but are coupled through a closed state. Histograms of channel residence times in the M and H states were found to be well described by a single exponential. The closed durations, however, were double exponentials and it was proposed that the two conducting units were coupled through the slow component of the distribution of closed durations.

Our analysis of the one-dimensional distributions shows that the M state has at least two components. The autocovariance functions indicate that the M state has at least two distinct entry/exit states. The transition history analysis illustrated with the box plots (Fig. 7) show that there is a structure in the transition history between the C, M, and H states. The main results are that as the voltage is made progressively more negative, the durations of M preceded and followed by H become shorter, while the durations in



M preceded and/or followed by C remain constant. The model suggested by Miller is inconsistent with our following findings: (a) the existence of two components in the distribution of dwell times in the M state; (b) the existence of autocovariance in the M lifetimes; (c) the dependence of the M lifetimes on the preceding and succeeding C and H states, as shown in Fig. 7.

In brief, we have identified not only the existence of two states in the M aggregate but established that the two states are kinetically distinguishable in the ways they communicate with the C and H aggregates. Our studies do not necessarily discard the idea proposed by Miller that the  $\text{Cl}^-$  channel is formed by two parallel subunits giving rise to the two conductance states. They do show, however, that these two open states are not identical or not independent.

In conclusion, autocorrelation analysis and transition history analysis provide a simple and general strategy to extract information on channel gating kinetics.

## APPENDIX

### Kinetic Schemes for the $\text{Cl}^-$ Channel

Miller (1982) considers a model of the  $\text{Cl}^-$  channel as a functional dimer consisting of two identical subunits (Fig. 9). These two subunits are linked through another closed state, D, resulting in the kinetic structure shown in Fig. 10. From Fig. 10 it is apparent that there is one entry state into C and H so that the autocorrelation functions for those aggregates should be null. Although there are two entry states into the M aggregate, the autocorrelation function for dwell times in this aggregate vanishes as well. To see this we construct the partitioned  $Q$  matrix for the underlying Markov process (for definitions see Colquhoun and Hawkes, 1981 or Fredkin et al., 1985)

$$Q = \begin{array}{c|ccccc} & \text{D} & \text{C}_1\text{C}_2 & \text{C}_1\text{O}_2 & \text{C}_2\text{O}_1 & \text{O}_1\text{O}_2 \\ \hline \text{D} & -\beta & \beta & 0 & 0 & 0 \\ \text{C}_1\text{C}_2 & \alpha & -(\alpha+2\lambda) & \lambda & \lambda & 0 \\ \text{C}_1\text{O}_2 & 0 & \mu & -(\mu+\lambda) & 0 & \lambda \\ \text{C}_2\text{O}_1 & 0 & \mu & 0 & -(\mu+\lambda) & \lambda \\ \text{O}_1\text{O}_2 & 0 & 0 & \mu & \mu & -2\mu \end{array} \quad (\text{A1})$$

$$= \begin{bmatrix} Q_{CC} & Q_{CM} & Q_{CH} \\ Q_{MC} & Q_{MM} & Q_{MH} \\ Q_{HC} & Q_{HM} & Q_{HH} \end{bmatrix} \quad (\text{A2})$$

The exponential decay parameters in the one-dimensional distribution of

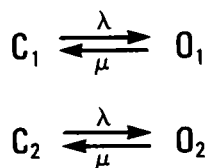


FIGURE 9 A model of the  $\text{Cl}^-$  channel with two independent, identical subunits (Miller, 1982), where C represents closed-channel states and O open states.

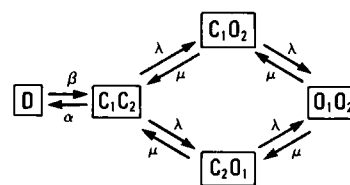


FIGURE 10 The kinetic scheme resulting from linking the subunits of Fig. 9 through an additional closed state D. The aggregate C consists of the states D and C<sub>1</sub>C<sub>2</sub>; M consists of C<sub>1</sub>O<sub>2</sub> and C<sub>2</sub>O<sub>1</sub>; H consists of O<sub>1</sub>O<sub>2</sub>.

dwell times in M are eigenvalues of  $Q_{MM}$ ; in the special case above both eigenvalues are equal to  $-(\mu + \lambda)$ , so that a single exponential appears.

From Theorem 5.1 of Fredkin et al., (1985) the number of components in the autocorrelation function of the M aggregate is  $\leq E - 1$  where

$$E = \text{rank } [Q_{MC} | Q_{MH}] \quad (\text{A3})$$

$$= \text{rank} \begin{bmatrix} 0 & \mu & \lambda \\ 0 & \mu & \lambda \end{bmatrix} \quad (\text{A4})$$

$$= 1. \quad (\text{A5})$$

(The rank of a matrix is the number of linearly independent columns.) Thus, Miller's model predicts a null correlation structure for the M aggregate. Note that if the subunits of Fig. 9 have different rate constants, the autocorrelation function of the M aggregate will not, in general, be null, and the one-dimensional distribution of dwell times in M will, in general, have two exponential components.

We thank Jon Lindstrom and Kee Wan for their continuous interest, and Richard Greenblatt and Yoav Blatt for comments on the manuscript.

This investigation was supported by research grants from the National Institutes of Health (EY-02084) and the Department of the Army Medical Research (DAMD17-82-C-2221) to M. Montal and the National Science Foundation (MCS 79-01800) and the National Institutes of Health (5R01 CA 2666-05) to J. Rice. During the course of this study P. Larbarca was a Muscular Dystrophy Association Fellow.

Received for publication 5 June 1984 and in final form 4 September 1984.

## REFERENCES

- Anholt, R., J. Lindstrom, M. Montal. 1981. Stabilization of acetylcholine receptor channels by lipids in cholate solution and during reconstitution in vesicles. *J. Biol. Chem.* 256:4377-4387.
- Anholt, R., D. R. Fredkin, T. Deerinck, M. Ellisman, M. Montal, and J. Lindstrom. 1982. Incorporation of acetylcholine receptors into liposomes: Vesicle structure and acetylcholine receptor function. *J. Biol. Chem.* 257:7122-7134.
- Anholt, R., J. Lindstrom, and M. Montal. 1984. The molecular basis of neurotransmission: Structure and function of the nicotinic acetylcholine receptor. In *The Enzymes of Biological Membranes*. A. Martonosi, editor. Plenum Publishing Corp., New York. Second ed. 3:335-401.
- Auerbach, A. and F. Sachs. 1984. Single channel currents from acetylcholine receptors in embryonic chick muscle. Kinetic and conductance properties of gaps within bursts. *Biophys. J.* 45:187-198.
- Becker, R. A. and J. M. Chambers. 1984. *An Interactive Environment for Data Analysis and Graphics*. Wadsworth Publishing Co., Belmont, CA.
- Boheim, G., W. Hanke, F. J. Barrantes, H. Eibl, B. Sakmann, G. Fels, and A. Maelicke. 1981. Agonist-activated ionic channels in acetylcholine receptor reconstituted into planar lipid bilayers. *Proc. Natl. Acad. Sci. USA.* 78:3586-3590.

- Changeux, J. -P. 1981. The acetylcholine receptor: An allosteric membrane protein. *Harvey Lect.* 75:85-254.
- Colquhoun, D., and A. G. Hawkes. 1981. On the stochastic properties of single ion channels. *Proc. R. Soc. Lond. B. Biol. Sci.* 211:205-235.
- Conti-Tronconi, B.M., and M. A. Raftery, 1982. The nicotinic cholinergic receptor: Correlation of molecular structure with functional properties. *Annu. Rev. Biochem.* 51:491-530.
- Cox, D. R., and P. A. W. Lewis. 1966. *The Statistical Analysis of Series of Events*. Methuen and Co. Ltd, London.
- Fredkin, D. R., M. Montal, and J. A. Rice. 1985. Identification of aggregated markovian models: Application to the nicotinic acetylcholine receptor. In *Proceedings of the Berkeley Conference in Honor of Jerzy Neyman and Jack Kiefer*. Wadsworth Publishing Co., Belmont, CA. In press.
- Hamill, O. P., and B. Sakmann. 1981. Multiple conductance states of single acetylcholine receptor channels in embryonic muscle cells. *Nature (Lond.)*. 294:462-464.
- Hamill, O., A. Marty, E. Neher, B. Sakmann, and F. J. Sigworth. 1981. Improved patch-clamp techniques for high resolution current recording from cells and cell-free patches. *Pfluegers Arch. Eur. J. Physiol.* 391:85-100.
- Hanke, W., and C. Miller. 1983. Single chloride channels from *Torpedo* electroplax: activation by protons. *J. Gen. Physiol.* 82:25-45.
- Huganir, R. L., M. A. Schell, and E. Racker. 1979. Reconstitution of the purified acetylcholine receptor from *Torpedo californica*. *FEBS (Fed. Eur. Biochem. Soc.) Lett.* 108:155-160.
- Jackson, M. B., B. S. Wong, C. E. Morris, H. Lecar, and C. N. Christian. 1983. Successive openings of the same acetylcholine receptor-channel are correlated in their open times. *Biophys. J.* 42:109-114.
- Karlin, A. 1983. Anatomy of a receptor. *Neurosci. Commentaries*. 3:111-123.
- Labarca, P., J. Lindstrom, M. Montal. 1984a. The acetylcholine receptor channel from *Torpedo californica* has two open states. *J. Neurosci.* 4:502-507.
- Labarca, P., J. Lindstrom, M. Montal. 1984b. Acetylcholine receptor in planar lipid bilayers. Characterization of the channel properties of the purified nicotinic receptor from *Torpedo californica* reconstituted in planar lipid bilayers. *J. Gen. Physiol.* 83:473-496.
- Labarca, P., J. Rice, J. Lindstrom, and M. Montal. 1984c. Covariance analysis of single channel currents from purified acetylcholine receptor and chloride channels in planar lipid bilayers. *Biophys. J.* 45(2, Pt. 2):387a. (Abstr.)
- Merril, C. R., D. Goldman, S. A. Sedman, and M. H. Ebert. 1981. Ultrasensitive stain for proteins in polyacrylamide gels shows regional variation in cerebrospinal fluid proteins. *Science (Wash.)*. 211:1437-1438.
- Miller, C., and M. M. White. 1980. A voltage-gated  $\text{Cl}^-$  conductance channel from *Torpedo* electroplax membrane. *Ann. NY Acad. Sci.* 341:534-551.
- Miller, C. 1982. Open-state substructure of single chloride channels from *Torpedo* electroplax. *Phil. Trans. R. Soc. Lond. B. Biol. Sci.* 299:401-411.
- Miller, C., and M. M. White. 1984. Dimeric structure of single chloride channels from *Torpedo* electroplax. *Proc. Natl. Acad. Sci. USA*. 81:2772-2775.
- Montal, M. 1974. Formation of bimolecular membranes from lipid monolayers. *Methods Enzymol.* 32:545-556.
- Montal, M., A. Darszon, and H. Schindler. 1981. Functional reassembly of membrane proteins in planar lipid bilayers. *Q. Rev. Biophys.* 14:1-79.
- Nelson, N., R. Anholt, J. Lindstrom, and M. Montal. 1980. Reconstitution of purified acetylcholine receptors with functional ion channels in planar lipid bilayers. *Proc. Natl. Acad. Sci. USA*. 77:3057-3061.
- Schindler, H., and U. Quast. 1980. Functional acetylcholine receptor from *Torpedo marmorata* in planar membranes. *Proc. Natl. Acad. Sci. USA*. 77:3052-3056.
- Suarez-Isla, B. A., K. Wan, J. Lindstrom, and M. Montal. 1983. Single-channel recordings from purified acetylcholine receptors reconstituted in bilayers formed at the tip of patch pipets. *Biochemistry*. 22:2319-2323.
- Tank, D. W., C. Miller, and W. W. Webb. 1982. Isolated patch recording from liposomes containing functionally reconstituted chloride channels from *Torpedo* electroplax. *Proc. Natl. Acad. Sci. USA*. 79:7749-7753.
- White, M. M., and C. Miller. 1979. A voltage-gated anion channel from the electric organ of *Torpedo californica*. *J. Biol. Chem.* 254:10161-10166.
- White, M. M., and C. Miller. 1981. Probes of the conduction process of a voltage gated  $\text{Cl}^-$  channel from *Torpedo* electroplax. *J. Gen. Physiol.* 78:1-18.